

Spectroscopy of mixed early–late transition metal diatomics: ScNi, YPd, and ZrCo

Caleb A. Arrington and Michael D. Morse

Department of Chemistry, University of Utah, Salt Lake City, Utah 84112

Mats Doverstål

Department of Physics, Stockholm University, Vanadisvägen 9, 11346 Stockholm, Sweden

(Received 4 October 1994; accepted 27 October 1994)

Resonant two-photon ionization spectroscopy has been employed to investigate the spectra of the jet-cooled transition metal diatomics ScNi, YPd, and ZrCo, which are isovalent species which possess (or are thought to possess) an $X^2\Sigma^+$ ground state. Several electronic band systems have been observed for these species in the near infrared, and the analysis of these systems is reported. Ground state vibrational intervals of $\Delta G''_{1/2} = 334.5 \pm 1.0$, 264.4 ± 0.2 , and 357.7 cm^{-1} have been determined for ScNi, YPd, and ZrCo, respectively. The spectroscopic results obtained for ScNi and YPd are compared to theoretical calculations performed by other researchers, and a discussion of the chemical bonding in these species is presented. © 1995 American Institute of Physics.

I. INTRODUCTION

The isovalent transition metal diatomics ScNi, YPd, and ZrCo belong to the category of mixed early–late transition metal dimers, created by taking one atom from the left side and one from the right side of the transition metal series. Such compounds have been postulated by Brewer and Engel to be particularly stable because of a partial donation of s electron density from the early to the late transition metal atom, balanced by back donation of d electron density from the late to the early transition metal atom.¹ The back donation of d electron density has been postulated to lead to strong d -orbital bonding in these species, and it has indeed been observed that the early–late intermetallic compounds YCo, YNi, ZrCo, ZrNi, NbCo, and NbNi are substantially more strongly bound than are the homonuclear molecules Co_2 , Ni_2 , and Y_2 (although comparable in bond strength to Zr_2 and more weakly bound than Nb_2).² Nevertheless, recent *ab initio* studies of ZrPt have cast the Brewer–Engel model of bonding into doubt.³ With this in mind we have undertaken a spectroscopic study of ScNi, YPd, and ZrCo to obtain further experimental data relevant to the bonding in these early–late transition metal diatomic molecules.

The ScNi, YPd, and ZrCo molecules contain thirteen valence ($d+s$) electrons and are thought to share a common $2\Sigma^+$ ground state. Such 13 electron transition metal diatomics are among the best studied of the mixed transition metal dimers, with Weltner's group having reported matrix isolation electron spin resonance (ESR) spectra for ScNi,⁴ ScPd,⁵ TiCo,⁴ YNi,⁵ and YPd,⁵ all of which have been shown to possess 2Σ ground states. On the theoretical side, an early all-electron Hartree–Fock calculation on YPd⁶ has been superseded by high-quality correlated *ab initio* studies of ScNi, YNi, ScPd, and YPd by Faegri and Bauschlicher.⁷ These complete active space self-consistent field multireference configuration interaction (CASSCF-MRCI) calculations predict $2\Sigma^+$ ground states for all four molecules, and excited electronic states are also reported, with particular emphasis placed on the electronic states of YPd. More recently, Mattar and Hamilton have reported local-density functional linear

combination of atomic orbital (LDF-LCAO) computations on ScNi and have included predictions of low-lying excited electronic states as well.⁸ Through the combination of the present spectroscopic study of these molecules and the previous ESR and theoretical investigations, a more detailed understanding of these complicated transition metal molecules may be gained.

In their ESR studies Van Zee and Weltner have shown that the ground $2\Sigma^+$ states of ScNi, ScPd, YNi, and YPd all possess g values shifted only slightly lower than 2.0023 (the value of the free electron), indicating that the ground state in these metal diatomics is a nearly unperturbed 2Σ state.⁵ The measured hyperfine splittings indicate that the majority of the unpaired spin resides on the early transition metal atom with both isotropic (s) and dipolar (presumed d , but possibly p) character. Further insight into the chemical bonding in these molecules has been derived through the theoretical studies of Faegri and Bauschlicher.⁷ In this work it is found that the ground state of all four molecules (ScNi, ScPd, YNi, and YPd) results from a combination of the atomic asymptotes of $d^1s^2, ^2D + d^{10}, ^1S$ (leading to a bond dominated by s electron donation from the early metal to the late metal) and $d^1s^2, ^2D + d^9s^1, ^3D$ (leading to a somewhat disfavored $\sigma^2\sigma^{*1}$ configuration in the s orbital space, but allowing the formation of a two-electron $d-d$ bond). Configuration interaction between these two states leads to the stabilization of a ground $2\Sigma^+$ state in all instances, regardless of the ordering of the atomic asymptotes. In addition to their study of the ground state bonding in these molecules, Faegri and Bauschlicher have calculated several excited state potential energy surfaces in YPd up to $20\,000 \text{ cm}^{-1}$, “in order to aid in the interpretation of any future spectroscopic study.”⁷ The present investigation was begun largely as a result of these words of enticement to the experimental spectroscopist.

Section II describes the experimental techniques employed in this study; spectroscopic results on ScNi, YPd, and ZrCo are presented in Sec. III. In Sec. IV a discussion of the chemical bonding of these mixed-metal molecules is pro-

vided, and Sec. V summarizes the most important results from this work.

II. EXPERIMENT

Jet-cooled molecular beams containing gaseous ScNi, YPd, and ZrCo molecules were produced by pulsed laser ablation (Nd:YAG, 532 nm, 20 mJ per pulse) of an alloy disk of the appropriate metal mixture in the throat of a pulsed supersonic expansion of helium. The alloy used in the production of ScNi was a triple mixture of Sc, Ni, and Cu metals in a 1:1:1 mole ratio purchased from Rhône-Poulenc. For production of diatomic YPd and ZrCo, equimolar Y:Pd and Zr:Co alloy sample disks were prepared in house using a Centaur electric arc furnace. Preweighed samples of the individual metals were melted in the electric arc (200 amp 40 V) under an argon atmosphere, cooled, and lathed to flatness. The resulting disks appeared to be homogeneous samples, and were suitable for use in laser ablation experiments using a resonant two-photon ionization spectrometer which has been previously described.⁹

The mixed-metal plasma generated by pulsed laser vaporization was created at the peak density of a helium carrier gas pulse traveling over the surface of the target disk, thus entraining the metal plasma in the carrier gas. Clustering of the metals was allowed to occur along a 2 mm diameter, 3 cm long channel prior to supersonic expansion from a 2 mm exit orifice. In the ensuing expansion from a 120 psi helium reservoir pressure to a chamber pressure of 6×10^{-4} Torr the internal degrees of freedom of the metal clusters were cooled substantially. The resulting jet-cooled molecular beam was roughly collimated by a 5 mm diameter skimmer 15 cm downstream from the expansion orifice, which admitted the molecular beam into the ionization region of a reflectron time-of-flight mass spectrometer.

In this second chamber the molecular beam was excited using radiation from a Nd:YAG pumped tunable dye laser, which was counterpropagated along the molecular beam. Timed so that the molecules were still in an excited state, a pulsed excimer laser operating on KrF (248 nm 5.00 eV) was fired across the molecular beam, ionizing the excited molecules. The ions created in this manner were accelerated into a reflectron time-of-flight mass spectrometer, with ion detection accomplished using a dual microchannel plate detector. The resulting signal was preamplified and digitized, following which it was further processed, stored, and displayed using a DEC LSI-11/73 microcomputer. A mass-resolved optical spectrum was thus recorded by monitoring mass-resolved ion signal as a function of the dye laser excitation frequency.

Bands in ScNi, YPd, and ZrCo were examined under high resolution (0.04 cm^{-1}) in the hope of obtaining rotationally resolved spectra. Unfortunately, rotational structure could not be resolved in any of these molecules, but an accurate calibration of the dye laser was achieved. The output of the dye laser was narrowed by employing an air-spaced intracavity étalon, which was pressure scanned with DuPont Freon 12. The resulting narrow-linewidth radiation was used to simultaneously record an absorption spectrum of gas phase I_2 along with the spectrum of the diatomic metal. The

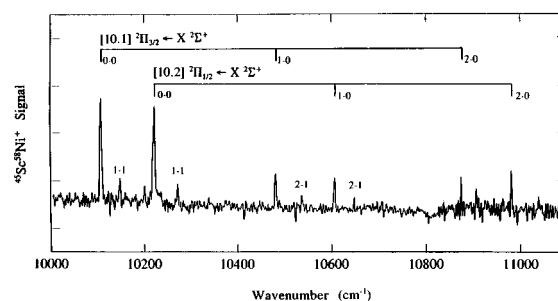


FIG. 1. Low resolution resonant two-photon ionization spectrum of the $[10.1]^2\Pi \leftarrow X^2\Sigma^+$ band system of diatomic $^{45}\text{Sc}^{58}\text{Ni}$. The spectrum was collected using Raman shifted Stokes radiation from laser dyes LDS 698 and DCM for photoexcitation followed by KrF excimer radiation for photoionization.

I_2 absorption spectrum was calibrated using the I_2 atlas of Gerstenkorn and Luc.¹⁰ As a result, all reported band positions are thought to be correct to within 2 cm^{-1} , the accuracy with which ν_0 can be determined from the band profile.

Excited state lifetimes were measured by the time-delayed resonant two-photon ionization technique. The resulting decay curves were fit to an exponential decay function by a nonlinear least-squares method,¹¹ allowing the upper state lifetimes to be extracted.

III. RESULTS

Although these studies did not result in rotationally resolved spectra, low resolution (0.8 cm^{-1}) spectra recorded for ScNi, YPd, and ZrCo, when examined in conjunction with theoretical calculations, provide new spectroscopic information about these mixed-metal diatomics.

A. ScNi

The optical spectrum of ScNi was investigated throughout the energy range $10\,000\text{--}24\,000 \text{ cm}^{-1}$. Although a very broad range was investigated, only a single band system was found. This band system, labeled the $[10.1]^2\Pi \leftarrow X^2\Sigma^+$ system, is displayed in Fig. 1, which was recorded using the Stokes radiation produced using the H_2 stimulated Raman scattering¹² of laser dyes LDS 698 and DCM for photoexcitation, and KrF excimer radiation (248 nm, 5.00 eV) for photoionization. The stimulated Raman scattering process occurs only on the $Q(1)$ line, resulting in a precise frequency shift of 4155.163 cm^{-1} when a hydrogen gas pressure of 500 psi is employed.

It is unfortunate that we were unable to rotationally resolve this band system to provide rotational constants, bond lengths, and upper state Ω values. Nevertheless, a distinguishing feature in the spectrum makes its assignment as a $^2\Pi \leftarrow X^2\Sigma^+$ system definite. This is the presence of two subsystems of nearly identical intensity, which indicates that transitions from a single substrate in the lower electronic state are terminating on two different spin-orbit levels of the upper state. Given that the ground state is known to be $^2\Sigma^+$ from the work of Van Zee and Weltner,⁵ Faegri and Bauschlicher,⁷ and Mattar and Hamilton,⁸ the only electric dipole-allowed transitions which are possible are

${}^2\Sigma^+ \leftarrow X {}^2\Sigma^+$ and ${}^2\Pi \leftarrow X {}^2\Sigma^+$. The former possibility would lead to only a single band system, while the latter would give two subsystems, ${}^2\Pi_{1/2} \leftarrow X {}^2\Sigma^+$ and ${}^2\Pi_{3/2} \leftarrow X {}^2\Sigma^+$, separated by the spin-orbit interval in the excited ${}^2\Pi$ state. On this basis the upper state may be assigned as a ${}^2\Pi$ state, although we have no definitive means of assigning the Ω components. (A tentative assignment based on band contours is given below.) For the present, the upper states are designated the $[10.1]{}^2\Pi_L$ and $[10.2]{}^2\Pi_U$ states (indicating the lower and upper spin-orbit component, respectively). In any case, the existence of an excited ${}^2\Pi$ state in this energy region is in agreement with the LDF-LCAO calculations of Mattar and Hamilton,⁸ who predict the second state of ${}^2\Pi$ symmetry to lie at $11\,331\text{ cm}^{-1}$, only $\approx 1\,200\text{ cm}^{-1}$ above the experimental location of the observed $[10.1]{}^2\Pi$ state.

The $[10.1]{}^2\Pi_L \leftarrow X {}^2\Sigma^+$ and $[10.2]{}^2\Pi_U \leftarrow X {}^2\Sigma^+$ subbands, listed in Table I, were fit as separate band systems using the standard expression,

$$\nu = T_0 + \omega'_e v' - \omega'_e x'_e (v'^2 + v') - \Delta G''_{1/2} v'', \quad (3.1)$$

for $v'' = 0$ or 1 . Fitted spectroscopic constants for this and all other band systems are given in Table II. The $[10.2]{}^2\Pi_U \leftarrow X {}^2\Sigma^+$ progression fits the formula quite adequately, accounting for all of the observed transitions to better than 1 cm^{-1} accuracy. This is not true of the $[10.1]{}^2\Pi_L \leftarrow X {}^2\Sigma^+$ progression, however, which requires the exclusion of either the $v' = 1$ or $v' = 2$ level to achieve a reasonable fit. The need to exclude an excited state vibrational level is indicative of a strong perturbation, however, with only three excited state levels optically accessible it is difficult to determine which level is perturbed. The constants obtained for the $[10.2]{}^2\Pi_U \leftarrow X {}^2\Sigma^+$ progression are $\Delta G''_{1/2} = 334.6 \pm 0.7\text{ cm}^{-1}$, $\omega'_e = 391.2 \pm 2.2\text{ cm}^{-1}$, and $\omega'_e x'_e = 3.41 \pm 0.71\text{ cm}^{-1}$ for ${}^{45}\text{Sc}^{58}\text{Ni}$. Without excluding any observed transitions the fit of the perturbed $[10.1]{}^2\Pi_L \leftarrow X {}^2\Sigma^+$ system gives values of $\Delta G''_{1/2} = 343.2 \pm 10.3\text{ cm}^{-1}$, $\omega'_e = 383.8 \pm 18.8\text{ cm}^{-1}$, and $\omega'_e x'_e = 0.37 \pm 4.55\text{ cm}^{-1}$ for ${}^{45}\text{Sc}^{58}\text{Ni}$, where the perturbation is responsible for the large errors in the fit. The ground state vibrational interval, $\Delta G''_{1/2}$, is of necessity the same regardless of the excited state accessed, so the best value is obtained as an average of the measured intervals between the $v' = 0$ and $v' = 1$ bands, providing $\Delta G''_{1/2} = 334.5 \pm 1.0\text{ cm}^{-1}$ for ${}^{45}\text{Sc}^{58}\text{Ni}$.

Although the lack of rotational resolution prevented a measurement of the rotational constants and a definitive assignment of the excited ${}^2\Pi$ state Ω values, information from the rotational contour suggests an assignment. Figure 2 displays the result of a slow low-resolution scan over the 0–0 bands of both the $[10.1]{}^2\Pi_L \leftarrow X {}^2\Sigma^+$ and the $[10.2]{}^2\Pi_U \leftarrow X {}^2\Sigma^+$ system. It is evident that the 0–0 band of the $[10.1]{}^2\Pi_L \leftarrow X {}^2\Sigma^+$ system displays a larger gap near the band origin than does the corresponding band of the $[10.2]{}^2\Pi_U \leftarrow X {}^2\Sigma^+$ system. This suggests that the proper designations of the $[10.1]{}^2\Pi_L$ and $[10.2]{}^2\Pi_U$ states are $[10.1]{}^2\Pi_{3/2}$ and $[10.2]{}^2\Pi_{1/2}$, respectively, since a ${}^2\Pi_{3/2} \leftarrow X {}^2\Sigma^+$ band will lack the $P_2(2)$, $P_{21}(1)$, $Q_2(1)$, and $Q_{21}(0)$ lines (labeled by N''), while the corresponding

$P_{12}(2)$, $P_1(1)$, $Q_{12}(1)$, and $Q_1(0)$ lines of the ${}^2\Pi_{1/2} \leftarrow X {}^2\Sigma^+$ band will be present and located near the band origin. On this basis a larger central dip in the band contour may be expected in the ${}^2\Pi_{3/2} \leftarrow X {}^2\Sigma^+$ band than in the ${}^2\Pi_{1/2} \leftarrow X {}^2\Sigma^+$ band, leading us to the tentative conclusion that the $[10.1]{}^2\Pi$ state is inverted. The same conclusion is reached upon examining a slow, low-resolution scan over the 1–0 bands.

The tentative assignment, based on band contour arguments, that the $[10.1]{}^2\Pi$ state is inverted runs counter to the theoretical results of Mattar and Hamilton.⁸ These authors calculate an excited ${}^2\Pi$ state of ScNi at $11\,331\text{ cm}^{-1}$, but find that it derives from the promotion of the unpaired σ electron in the ground state to an empty π orbital which is 82% $4p_{\text{Sc}}$, 16% $4p_{\text{Ni}}$, and 2% $3d_{\text{Sc}}$ in character.⁸ A ${}^2\Pi$ state resulting from such a π^1 configuration would normally be expected to be regular, with the ${}^2\Pi_{1/2}$ level lying below the ${}^2\Pi_{3/2}$ level, unless a serious perturbation were occurring. Although the vibrational structure of the $[10.1]{}^2\Pi_L$ state is clearly perturbed, it seems unlikely that the perturbation is sufficient to completely reverse the sense of the spin-orbit splitting. Clearly, further experimental and theoretical study will be required to resolve this question.

The lifetime of the $[10.1]{}^2\Pi$ state is measured by the time-delayed resonant two-photon ionization method to be $830 \pm 90\text{ ns}$. Assuming that the decay is dominated by fluorescence to the ground electronic state this corresponds to an absorption oscillator strength of $f \approx 0.016$, indicating a fairly strong electronic transition.

The isovalent species YNi displays a congested vibronic spectrum with an abrupt predissociation threshold which has been used to measure the bond dissociation energy, yielding $D_0(\text{YNi}) = 2.904 \pm 0.001\text{ eV}$.² It is quite surprising that a correspondingly congested vibronic spectrum is not evident in the case of ScNi. For reasons unknown, however, the band system displayed in Fig. 1 provides the only spectral features apparent in the range of $10\,000$ – $24\,000\text{ cm}^{-1}$. On the basis of the last observed Sc band of this system, at $10\,983\text{ cm}^{-1}$, the bond strength of ScNi may be assumed to be greater than 1.36 eV . By comparison to the bond strengths of the isovalent species YNi [$D_0(\text{YNi}) = 2.904 \pm 0.001\text{ eV}$]² and TiCo [$D_0(\text{TiCo}) = 2.401 \pm 0.001\text{ eV}$],¹³ however, a bond strength in excess of 2 eV would be expected.

B. YPd

The low resolution spectrum of YPd has been recorded from $18\,400$ to $6\,300\text{ cm}^{-1}$, revealing five band systems or subsystems. The determination by Van Zee and Weltner⁵ of the YPd ground state as ${}^2\Sigma^+$ greatly simplifies the optical spectroscopy, because the only electric dipole allowed Hund's case (a) transitions are ${}^2\Sigma^+ \leftarrow {}^2\Sigma^+$ and ${}^2\Pi \leftarrow {}^2\Sigma^+$. These two possibilities may be distinguished even in low resolution because the ${}^2\Pi$ state has two spin-orbit components, $\Omega = 1/2$ and $\Omega = 3/2$, which result in two allowed vibronic progressions at similar energies, as were observed for ScNi. In contrast, ${}^2\Sigma^+ \leftarrow {}^2\Sigma^+$ transitions will display only a single vibronic progression.

This simple method of assigning the excited state term symbol becomes more problematic when the molecule does

TABLE I. Vibronic bands of ScNi, YPd, and ZrCo.

System	Band	Observed frequency (cm ⁻¹) ^a	Isotope shift (cm ⁻¹)	Lifetime (μ s)
⁴⁵ Sc ⁵⁸ Ni ^{b,c} [10.1] ² Π _{3/2} ←X ² Σ ⁺	0-0	10 106.05(1.86)	0.08	
	1-0	10 479.89(-7.42)	-4.86	
	2-0	10 875.26(5.57)		
	1-1	10 145.99(1.86)	4.01	
	3-1	10 906.30(-1.86)		
⁴⁵ Sc ⁵⁸ Ni ^b [10.2] ² Π _{1/2} ←X ² Σ ⁺	0-0	10 220.52(0.20)	0.49	0.894±0.033
	1-0	10 604.04(-0.65)	-2.88	
	2-0	10 982.68(0.45)		
	0-1	9 885.49(-0.20)		
	1-1	10 270.69(0.65)		
⁸⁹ Y ¹⁰⁸ Pd ^d [6.5]←X ² Σ ⁺	0-0	6 456.76(0.11)	0.04	
	1-0	6 683.38(-0.33)	-0.96	
	2-0	6 910.70(0.22)	-1.85	
	2-1	6 647.72(0.11)	-0.24	
	3-1	6 873.95(-0.11)	-1.69	
⁸⁹ Y ¹⁰⁸ Pd ^d [6.9]←X ² Σ ⁺	0-0	6 945.28	0.03	
⁸⁹ Y ¹⁰⁸ Pd ^{d,e} [8.3]←X ² Σ ⁺	0-0	8 288.16(-0.36)	-0.03	
	1-0	8 526.64(1.15)	-1.05	
	2-0	8 757.57(-0.03)	-1.44	
	3-0	8 984.29(-0.58)	-2.71	
	4-0	9 207.26(-0.05)	-3.55	1.93 ±0.23
	5-0	9 425.25(0.35)	-4.73	
	6-0	9 637.23(-0.42)	-5.47	
	7-0	9 839.28 ^e	-6.06	
	8-0	10 048.59(-0.04)	-5.19	1.70 ±0.32
	3-1	8 719.61(-1.07)	-1.96	
	4-1	8 943.35(0.24)	-2.86	
	5-1	9 160.72(0.02)	-4.43	
	6-1	9 374.60(1.15)	-4.16	
⁸⁹ Y ¹⁰⁸ Pd ^d [10.4]←X ² Σ ⁺	7-1	9 574.13 ^e	-4.48	
	8-1	9 784.10(-0.33)	-4.09	
	0-0	10 378.96(-0.20)	-0.10	1.78 ±0.40
	1-0	10 657.03(-0.07)	-1.24	1.61 ±0.48
	2-0	10 934.07(-0.62)	-2.51	2.13 ±0.37
	3-0	11 212.82(0.89)		
	0-1	10 114.54(0.02)	1.15	
	1-1	10 393.08(0.61)	-0.68	
⁸⁹ Y ¹⁰⁸ Pd ^d (3) ² Σ ⁺ ←X ² Σ ⁺	2-1	10 670.14(0.08)	-0.97	
	3-1	10 946.60(-0.71)	-2.92	
	0-0	14 384.09(0.38)	-0.05	0.220±0.034
	1-0	14 588.94(-0.19)	-0.79	0.168±0.020
	2-0	14 793.90(0.21)	-0.60	0.160±0.082
	3-0	14 997.37(0.00)	-2.15	
	4-0	15 198.90(-1.28)	-3.96	0.141±0.038
	5-0	15 400.98(-1.13)	-4.93	0.163±0.023
	6-0	15 603.93(0.75)	-4.93	
	7-0	15 804.47(1.10)	-5.64	
	8-0	16 002.84(0.16)	-5.86	
	4-1	14 935.35(0.27)	-1.65	
	5-1	15 136.95(-0.07)	-2.85	
	6-1	15 338.33(0.26)	-4.30	
7-1	15 538.84(0.58)	-4.30		
8-1	15 737.22(-0.36)	-6.34		
9-1	15 935.63(-0.40)	-6.95		
10-1	16 133.30(-0.28)	...		

TABLE I. (Continued.)

System	Band	Observed frequency (cm ⁻¹) ^a	Isotope shift (cm ⁻¹)	Lifetime (μs)
⁹⁰ Zr ⁵⁹ Co ^{f,g} [10.5] ² Σ ⁺ ← X ² Σ ⁺	0-0	10 497.37	-1.11	0.516 ± 0.033
	1-0	10 888.45	-3.77	0.606 ± 0.016
	1-1	10 530.79	-0.88	
	2-1	10 915.09	-4.01	0.643 ± 0.070

^aMeasured vibronic bands positions were fit to the formula

$$\nu = T_0 + \omega'_e v' - \omega'_e x'_e (v'^2 + v') - \Delta G''_{1/2} v''$$

providing the values of ω'_e , $\omega'_e x'_e$, and $\Delta G''_{1/2}$ listed in Table II. Residuals ($\nu_{\text{obs}} - \nu_{\text{calc.}}$) are provided in units of cm⁻¹ in parentheses following each entry.

^bThe isotope shift is reported as $\nu(^{45}\text{Sc}^{60}\text{Ni}) - \nu(^{45}\text{Sc}^{58}\text{Ni})$.

^cThe poor vibration fit in the [10.2]²Π ← X²Σ⁺ band system indicates the presence of a significantly perturbed excited state vibrational level.

^dThe isotope shift is reported as $\nu(^{89}\text{Y}^{108}\text{Pd}) - \nu(^{89}\text{Y}^{106}\text{Pd})$.

^eThe $v' = 7$ level of the [8.3] state of YPd fits poorly into the progression and is apparently perturbed. Accordingly, both the 7-0 and 7-1 bands have been omitted from the fit.

^fThe isotope shift is reported as $\nu(^{94}\text{Zr}^{59}\text{Co}) - \nu(^{90}\text{Zr}^{59}\text{Co})$.

^gThe band system in ⁹⁰Zr⁵⁹Co was fit to the formula

$$\nu = T_0 + \Delta G'_{1/2} v' - \Delta G''_{1/2} v''.$$

not conform to pure Hund's case (a) behavior, however. For example, ²Δ_{3/2} excited states can mix with ²Π_{3/2} states via spin-orbit interactions, making the ²Δ_{3/2} ← X²Σ⁺ transition

TABLE II. Spectroscopic constants for ScNi, YPd, and ZrCo.^a

Molecule	State	Fitted constants	Lifetime ^b
⁴⁵ Sc ⁵⁸ Ni	[10.2] ² Π _{1/2}	$T_0 = 10\,220.33 \pm 0.67$ $\omega'_e = 391.17 \pm 2.16$ $\omega'_e x'_e = 3.41 \pm 0.71$	0.89 ± 0.03 μs
	[10.1] ² Π _{3/2}	$T_0 = 10\,102.46 \pm 8.03$ $\omega'_e = 384.60 \pm 6.22$ $\Delta G''_{1/2} = 334.5 \pm 1.0$	
	X ² Σ ⁺		
⁸⁹ Y ¹⁰⁸ Pd	(3) ² Σ ⁺	$T_0 = 14\,383.70 \pm 0.52$ $\omega'_e = 206.30 \pm 0.24$ $\omega'_e x'_e = 0.44 \pm 0.02$	170 ± 13 ns
	[10.4]	$T_0 = 10\,379.15 \pm 0.56$ $\omega'_e = 278.29 \pm 1.05$ $\omega'_e x'_e = 0.17 \pm 0.26$	1.88 ± 0.24 μs
	[8.3]	$T_0 = 8288.52 \pm 0.58$ $\omega'_e = 241.80 \pm 0.34$ $\omega'_e x'_e = 2.42 \pm 0.03$	1.85 ± 0.19 μs
	[6.9]	$T_0 = 6945.28$	
	[6.5]	$T_0 = 6456.65 \pm 0.43$ $\omega'_e = 227.38 \pm 0.82$ $\omega'_e x'_e = 0.15 \pm 0.21$ $\Delta G''_{1/2} = 264.39 \pm 0.24$	
	X ² Σ ⁺		
⁹⁰ Zr ⁵⁹ Co	[10.5] ² Σ ⁺	$T_0 = 10\,497.37$ $\omega'_e = 397.85$ $\omega'_e x'_e = 3.39$ $\Delta G''_{1/2} = 357.67$	0.59 ± 0.02 μs
	X ² Σ ⁺		

^aAll values are reported in wave numbers (cm⁻¹), errors represent a 1σ limit.

^bLifetimes are the result of a weighted average of several bands in the excited state system. No excited state system demonstrated a significant vibrational dependence in the lifetime. Errors reported represent 1σ in the nonlinear least squares fit.

weakly allowed. As a result both ²Σ⁺ and ²Δ states will appear as single vibrational progressions and will be indistinguishable under low resolution conditions. Likewise, if the spin-orbit interval in an excited ²Π state is sufficiently large, particularly if the Ω = 1/2 and 3/2 states are mixed with other states by spin-orbit interactions, it may be difficult to identify two progressions as belonging to the same ²Π ← X²Σ⁺ band system. With these caveats in mind, some tentative identifications of the upper state symmetry species are still possible, particularly through comparisons with the *ab initio* work of Faegri and Bauschlicher.⁷

1. The 14 400 cm⁻¹ band system of YPd

The highest energy assignable vibronic progression in YPd was found in the region 14 300 to 16 200 cm⁻¹, and was recorded using DCM and LDS 698 dye laser radiation for photoexcitation in combination with KrF excimer radiation (248 nm, 5.00 eV) for photoionization. This single band system, shown in Fig. 3, has been labeled as the (3)²Σ⁺ ← X²Σ⁺ system by comparison with the excited

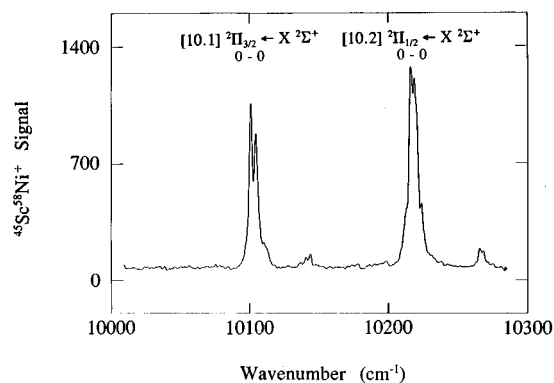


FIG. 2. Magnified low resolution scan over the 0-0 subbands of the [10.1]²Π_{3/2} ← X²Σ⁺ band system of ⁴⁵Sc⁵⁸Ni. The larger gap near the band origin in the 10 106 cm⁻¹ band suggests that it corresponds to the ²Π_{3/2} ← X²Σ⁺ 0-0 band, and that the [10.1]²Π state is inverted.

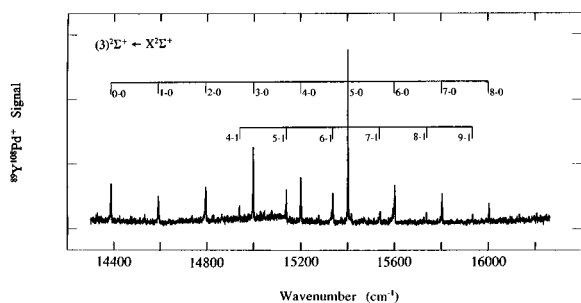


FIG. 3. Low resolution scan of the vibronic spectrum of $^{89}\text{Y}^{108}\text{Pd}$, recorded using LDS 698 and DCM dye laser radiation for excitation in conjunction with KrF radiation for photoionization. The $(3)^2\Sigma^+ \leftarrow X^2\Sigma^+$ vibrational progression is indicated.

state calculations of Faegri and Bauschlicher.⁷ These calculations employ a CASSCF-MRCI method including the multireference analog of the Davidson correction, which places the third state of $2\Sigma^+$ symmetry at $T_e = 15\,534\text{ cm}^{-1}$. The band system displayed in Fig. 3 is fitted very well by a vibrational model requiring only T_0 , ω'_e , $\omega'_e x'_e$, and $\Delta G''_{1/2}$, giving $T_0 = 14\,383.7 \pm 0.5\text{ cm}^{-1}$, corresponding to $T_e = 14\,413.2\text{ cm}^{-1}$. This falls well within the estimated uncertainty of $2\,000\text{ cm}^{-1}$ in the computed energies of the YPd excited states.⁷ In this same energy region, however, the second state of 2Δ symmetry is also calculated, and in the absence of rotationally resolved data we cannot with certainty rule out the possibility of $(2)^2\Delta_{3/2}$ as the excited state responsible for the observed band system. However, the transition moment calculated by Faegri and Bauschlicher for the $(3)^2\Sigma^+ \leftarrow X^2\Sigma^+$ transition is quite large (1.5 a.u.),⁷ implying that the $(3)^2\Sigma^+ \leftarrow X^2\Sigma^+$ system would be observed in our experiments. As the band system shown in Fig. 3 is the only band system observed in this energy region, it seems very likely that it does indeed correspond to the calculated $(3)^2\Sigma^+ \leftarrow X^2\Sigma^+$ system, and will be designated as such throughout the remainder of this paper.

It is evident in Fig. 3 that the 5–0 band (and possibly the 3–0 band as well) of the $(3)^2\Sigma^+ \leftarrow X^2\Sigma^+$ system of $^{89}\text{Y}^{108}\text{Pd}$ possesses an anomalously large intensity in the resonant two-photon ionization spectrum. This cannot be explained by Franck–Condon factors or by variations in the dye laser fluence as one scans across the gain profile of the dye. Instead, it reflects an enhanced probability of ionization at this wavelength, which is probably due to an accidental resonance for the absorption of a second dye laser photon at this frequency, followed by absorption of a third dye laser photon to ionize the molecule. Although this possibility was not explicitly tested by collection of a spectrum without KrF excimer radiation for photoionization, it nevertheless seems plausible. The observation of a vibrational 0–0 band at 6456.8 cm^{-1} (0.801 eV) in this molecule using KrF radiation ($40\,300\text{ cm}^{-1}$, 4.997 eV) for photoionization (see below) places the ionization energy below $46\,757\text{ cm}^{-1}$ (5.797 eV), while the three-photon process just described for the excitation of the 5–0 band requires that the ionization energy lie below $46\,203\text{ cm}^{-1}$ (5.728 eV). Given that the ionization energy is known to lie below 5.797 eV, it is plausible that it

also lies below 5.728 eV. Another observation supporting the suggested three-photon accidental resonance mechanism is the fact that other isotopic combinations of YPd display anomalous intensity in other vibrational bands of this system. In particular, $^{89}\text{Y}^{105}\text{Pd}$ displays a large enhancement in the 6–0 band, with a more moderate enhancement in the 5–0 band and $^{89}\text{Y}^{110}\text{Pd}$ displays a large enhancement in the 6–0 band with no apparent enhancement in the 5–0 band. If the three-photon accidental resonance mechanism is valid, isotopic shifts in the vibrational levels would be expected to bring different bands into three-photon resonance, leading to an isotopically variable pattern of anomalous band enhancements, as observed.

A fit of the observed vibrational bands to Eq. (3.1) provides constants for the band system of $T_0 = 14\,383.70 \pm 0.52\text{ cm}^{-1}$, $\omega'_e = 206.31 \pm 0.24\text{ cm}^{-1}$, $\omega'_e x'_e = 0.44 \pm 0.02\text{ cm}^{-1}$, and $\Delta G''_{1/2} = 265.10 \pm 0.42\text{ cm}^{-1}$ for $^{89}\text{Y}^{108}\text{Pd}$. Measured band positions are listed in Table I along with the residuals in the least-squares fit to Eq. (3.1). The vibrational interval measured for the ground state is in remarkable agreement with the theoretically predicted vibrational frequency of $\omega''_e = 259\text{ cm}^{-1}$,⁷ an indication of the accuracy of the theoretical description of the ground state bonding in YPd. As may be expected, however, this level of accuracy is not reproduced in the $(3)^2\Sigma^+$ excited state, where ω_e is predicted to be 269 cm^{-1} at the CASSCF-MRCI level, but increases to 333 cm^{-1} with the inclusion of the multireference equivalent of the Davidson correction.⁷ The large change of ω_e upon inclusion of the Davidson correction may be taken as evidence that an even more highly correlated calculation is required to accurately describe the potential energy surface of the $(3)^2\Sigma^+$ state of YPd.

Excited state lifetimes measured for members of the $(3)^2\Sigma^+ \leftarrow X^2\Sigma^+$ band system were all close to 160 ns. The lack of a significant vibrational dependence in the measured lifetimes strongly suggests that predissociation is not occurring in this band system. In addition, the calculations of Faegri and Bauschlicher predict that the $(3)^2\Sigma^+$ state lies below the lowest separated atom limit in YPd, which is predicted to be bound by 2.40 eV ($19\,350\text{ cm}^{-1}$) at the CASSCF-MRCI level including the analog of Davidson's correction.⁷ An experimental estimate of the YPd bond strength has also been made by Knudsen effusion methods, resulting in a selected value of $D_0^0(\text{YPd}) = 2.46 \pm 0.16\text{ eV}$ ($19\,800 \pm 1\,250\text{ cm}^{-1}$).¹⁴ These results are in good agreement and imply that the decay of the $(3)^2\Sigma^+$ state is due to fluorescence rather than predissociation. Assuming that this is dominated by fluorescence to the ground electronic state, the measured lifetime corresponds to an absorption oscillator strength of $f \approx 0.05$, which is in reasonable agreement with the oscillator strength ($f = 0.10$) derived from the calculated transition moment (1.5 a.u.)⁷ of the $(3)^2\Sigma^+ \leftarrow X^2\Sigma^+$ band system. The agreement between these values provides strong support for the identification of the observed band system as the $(3)^2\Sigma^+ \leftarrow X^2\Sigma^+$ system.

2. Near infrared band systems of YPd

The lower frequency band systems of YPd ($11\,000$ – $6\,500\text{ cm}^{-1}$) were recorded by Raman shifting the laser ra-

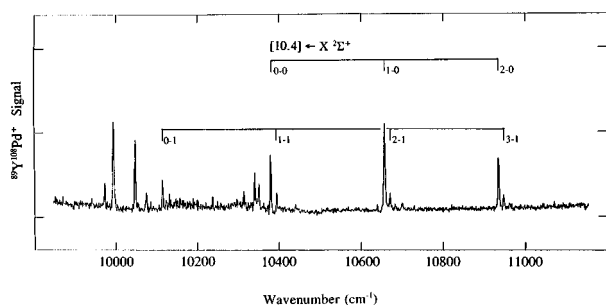


FIG. 4. Low resolution scan of the $[10.4] \leftarrow X^2\Sigma^+$ band system of $^{89}\text{Y}^{108}\text{Pd}$, recorded using the H_2 Raman shifted first Stokes radiation from laser dye LDS 698 and the fundamental radiation from laser dye LDS 925 in conjunction with KrF radiation for photoionization.

diation from dyes LDS 698, LDS 750, and LDS 751 using a cell pressurized with H_2 (500 psi) to produces first or second Stokes-shifted radiation lying 4155.163 or 8310.326 cm^{-1} lower in frequency than the fundamental laser radiation, respectively. Photoionization was again accomplished using 248 nm (5.00 eV) KrF excimer laser radiation.

It is difficult to make a one-to-one correspondence between the observed near infrared band systems and those calculated by Faegri and Bauschlicher.⁷ This is particularly true because these *ab initio* investigations have not included the spin-orbit interaction, which can be quite significant in palladium-containing compounds [$\zeta_{4d}(\text{Pd}) \approx 1495 \text{ cm}^{-1}$].¹⁵ The combination of this problem and our inability at the present time to rotationally resolve any of the systems (and thereby to identify the state symmetries) makes the comparison between theory and experiment tenuous at best.

The first of the band systems to be encountered as one scans further to the red is found in the range 10 100–11 200 cm^{-1} and is displayed in Fig. 4. A short progression up to the 3–0 band is found, which is fitted well to the expression of Eq. (3.1), yielding values of $T_0 = 10\,379.15 \pm 0.56 \text{ cm}^{-1}$, $\omega'_e = 278.29 \pm 1.05 \text{ cm}^{-1}$, $\omega'_e x'_e = 0.17 \pm 0.26 \text{ cm}^{-1}$, and $\Delta G''_{1/2} = 264.63 \pm 0.51 \text{ cm}^{-1}$ for $^{89}\text{Y}^{108}\text{Pd}$. This fitted value of the ground state vibrational interval is in excellent agreement with that found from the $(3)^2\Sigma^+ \leftarrow X^2\Sigma^+$ system. For purposes of discussion, this system will be designated the $[10.4] \leftarrow X^2\Sigma^+$ band system.

The next band system encountered as one moves to the red is found in the range 8 200–10 100 cm^{-1} and is displayed in Fig. 5. A long progression out to the 8–0 band is found. Apart from the 7–0 and 7–1 bands this is again fitted quite well to Eq. (3.1), yielding values of $T_0 = 8288.52 \pm 0.58 \text{ cm}^{-1}$, $\omega'_e = 241.80 \pm 0.34 \text{ cm}^{-1}$, $\omega'_e x'_e = 2.42 \pm 0.03 \text{ cm}^{-1}$, and $\Delta G''_{1/2} = 264.20 \pm 0.45 \text{ cm}^{-1}$ for $^{89}\text{Y}^{108}\text{Pd}$. Apparently, the $v' = 7$ level of the upper state is perturbed, although the perturber state is not in evidence. This system will be designated the $[8.3] \leftarrow X^2\Sigma^+$ band system.

Even further to the red one encounters the band system displayed in Fig. 6. This extremely low frequency band system was recorded using the second Stokes radiation from laser dyes LDS 698 and DCM, Raman shifted in H_2 . With the filters available in our laboratory it was possible to block

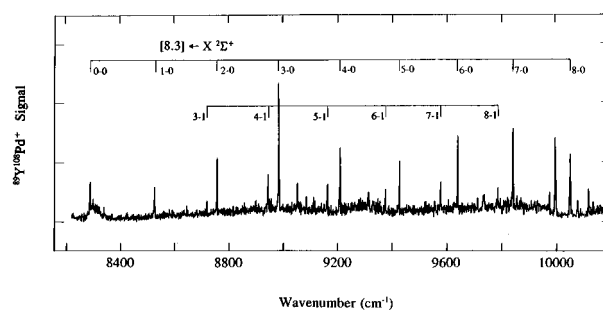


FIG. 5. A portion of the low resolution spectrum of $^{89}\text{Y}^{108}\text{Pd}$, recorded using first Stokes Raman shifted radiation from laser dyes LDS 698, LDS 750, and LDS 751, followed by KrF excimer radiation for photoionization. The labeled band system is designated as the $[8.3] \leftarrow X^2\Sigma^+$ system.

the second Stokes and the fundamental radiation while transmitting the first Stokes radiation or to block the fundamental while transmitting the first and second Stokes radiation. We were not, however, able to transmit the second Stokes radiation while blocking the fundamental and first Stokes radiation. As a result, bands which are excited by the first Stokes radiation are present in Fig. 6 and are indicated by asterisks. They correspond to vibronic bands of the $[10.4] \leftarrow X^2\Sigma^+$ band system described above, and are labeled with vibrational numbers in addition to the asterisks. As in the other band systems, this system is well described by Eq. (3.1), which yields values of $T_0 = 6456.65 \pm 0.43 \text{ cm}^{-1}$, $\omega'_e = 227.38 \pm 0.82 \text{ cm}^{-1}$, $\omega'_e x'_e = 0.15 \pm 0.21 \text{ cm}^{-1}$, and $\Delta G''_{1/2} = 262.87 \pm 0.62 \text{ cm}^{-1}$ for $^{89}\text{Y}^{108}\text{Pd}$. This will be designated the $[6.5] \leftarrow X^2\Sigma^+$ band system.

Finally, the strongest feature in the spectrum displayed in Fig. 6, a band induced by the second Stokes radiation at 6945 cm^{-1} , appears as a single feature without an attendant vibrational progression. Based on the measured isotope shift [$\nu(^{89}\text{Y}^{108}\text{Pd}) - \nu(^{89}\text{Y}^{106}\text{Pd}) = 0.026 \text{ cm}^{-1}$] this is vibrationally a 0–0 band and the absence of a progression suggests that the bond length remains nearly unchanged in the electronic

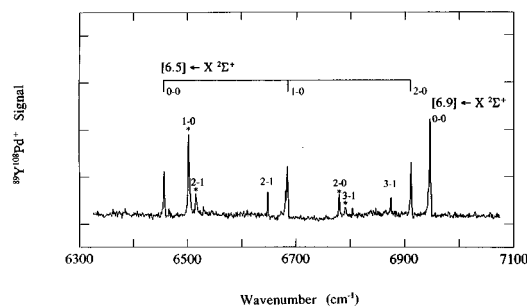


FIG. 6. Low resolution optical spectrum of the lowest frequency transitions of $^{89}\text{Y}^{108}\text{Pd}$. This resonant two-photon ionization spectrum was recorded using second Stokes radiation from the laser dyes LDS 698 and DCM, Raman shifted in high pressure H_2 for photoexcitation, followed by photoionization using KrF excimer radiation. Bands marked with asterisks (and labelled by vibrational numbers) derived from the $[10.4] \leftarrow X^2\Sigma^+$ band system and are excited with the first Stokes radiation, which was also present when this scan was recorded. Two band systems are apparent in this region, designated the $[6.5] \leftarrow X^2\Sigma^+$ and $[6.9] \leftarrow X^2\Sigma^+$ systems.

excitation. However, we have no way of verifying that the second Stokes radiation was produced over the entire range of dye laser frequencies, so it is possible that we were unable to access the spectroscopic region between 7000 and 8000 cm^{-1} . It is therefore possible that the 1–0 and higher members of the vibrational progression were not observed simply because the requisite second Stokes radiation was not produced. In any event, this band system will be designated the $[6.9] \leftarrow X^2\Sigma^+$ band system.

For all of the infrared band systems reported for YPd, the isotope shift between the $^{89}\text{Y}^{108}\text{Pd}$ and $^{89}\text{Y}^{106}\text{Pd}$ isotopic modifications (shown in Table I) provides strong support for the vibrational assignment. In addition, the observation of such low energy excited states places strong restrictions on the ionization energy, IE(YPd). The successful use of KrF radiation (4.997 eV) as the second photon in the R2PI scheme implies that $\text{IE}(\text{YPd}) > 4.997$ eV. The observation of the 0–0 band of the $[6.5] \leftarrow X^2\Sigma^+$ band system at 6457 cm^{-1} in turn places the ionization energy of YPd below 5.80 eV. Together these bracket the ionization energy as $\text{IE}(\text{YPd}) = 5.40 \pm 0.40$ eV. The possibility of observing such low energy transitions using KrF excimer radiation for photoionization is confirmed by the observation in our laboratory of a one-photon ionization threshold in YPd at 5.475 eV, placing $\text{IE}(\text{YPd}) = 5.475 \pm 0.001$ eV.¹⁶

In the near-infrared spectral region Bauschlicher and Faegri predict numerous excited electronic states.⁷ Predicted electronic term energies (T_e) of the states which are spectroscopically accessible under case (a) selection rules are 5 883 cm^{-1} [$^2\Pi$]; 7 100 cm^{-1} [$(2)^2\Sigma^+$]; and 10 820 cm^{-1} [$(2)^2\Pi$]. In addition, states which may become accessible through spin–orbit coupling are predicted with term energies (T_e) of 4 221 cm^{-1} [$^2\Delta$]; 10 947 cm^{-1} [$^4\Delta$]; 13 815 cm^{-1} [$^4\Pi$]; and 16 774 cm^{-1} [$(2)^2\Delta$]. The $[6.5] \leftarrow X^2\Sigma^+$ band system displayed in Fig. 6 is close to the predicted term energy of the $(2)^2\Sigma^+$ state, and the measured vibrational frequency of 227.4 cm^{-1} is quite close to the calculated value (223 cm^{-1}) as well. This suggests that the upper state of this system may indeed be $^2\Sigma^+$ in character, although this is not proven. In the absence of rotationally resolved and analyzed spectra it is even more problematic to identify the remaining band systems with those which are theoretically predicted. Further discussion of this comparison between theory and experiment must wait until more definitive experimental assignments are in hand.

C. ZrCo

As in the isovalent 13 valence electron transition metal molecules ScNi,^{4,7,8} TiCo,⁴ ScPd,^{5,7} YNi,^{5,7} and YPd,^{5,7} the ground state of ZrCo is presumably $^2\Sigma^+$, although to our knowledge this has not yet been experimentally verified or theoretically predicted. Although ZrCo does indeed possess the same number of valence electrons as ScNi, ScPd, YNi, and YPd, the addition of one electron to the early transition metal atom and the removal of one electron from the late transition metal atom dramatically alters the number of distinct relativistic adiabatic [Hund's case (c)] potential energy surfaces that arise from separated atom limits within 10 000 cm^{-1} of ground state atoms. In the examples of ScNi, ScPd,

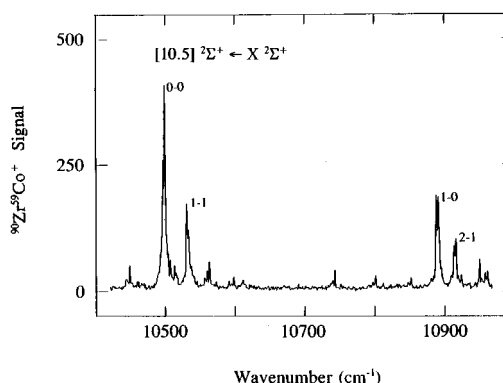


FIG. 7. Low resolution resonant two-photon ionization spectrum of a low energy band system in jet-cooled $^{90}\text{Zr}^{59}\text{Co}$, recorded using first Stokes radiation from laser dyes LDS 698 and DCM, Raman shifted in high pressure H_2 , in conjunction with KrF excimer radiation for photoionization. The strong features have been tentatively assigned as the $[10.5] \leftarrow X^2\Sigma^+$ band system.

YNi, and YPd the number of Hund's case (c) states arising within 10 000 cm^{-1} of ground state atoms are 205, 65, 205, and 65, respectively, while ZrCo generates 2055 Hund's case (c) states within 10 000 cm^{-1} of ground state atoms. This implies a much more complicated electronic structure and electronic spectrum in the case of ZrCo, and it may well be that this increased electronic complexity accounts for the lack of published reports on the molecule. Surely the increased number of low-lying electronic states in this molecule will simultaneously make configuration interaction more important and more difficult to properly include.

The increased density of electronic states in ZrCo is evidenced in the spectrum by a near-continuum of optical absorption throughout the visible and ultraviolet, culminating in an abrupt predissociation threshold at 25 298 cm^{-1} , which corresponds to the bond dissociation energy of the molecule.² In the near infrared region, which we have investigated down to 8830 cm^{-1} , however, only one isolated excited state has been observed using the resonant two-photon ionization method. This band system, displayed in Fig. 7, was recorded using laser dyes LDS 698 and DCM, Raman shifted in high pressure H_2 to produce Stokes-shifted radiation for excitation, which was used in combination with KrF excimer radiation (248 nm, 5.00 eV) for photoionization.

The band system is dominated by a strong feature at 10 497 cm^{-1} , which displays a small isotope shift [$\nu(^{94}\text{Zr}^{59}\text{Co}) - \nu(^{90}\text{Zr}^{59}\text{Co}) = -1.1$ cm^{-1}] consistent with its identification as an origin band. A weaker feature at 10 531 cm^{-1} also displays a small isotope shift, suggesting that it may be a 1–1 vibrational hot band. Near 10 900 cm^{-1} two additional weaker features display isotope shifts that are consistent with their identification as the 1–0 and 2–1 bands of the system. This assignment provides a good fit to Eq. (3.1), giving constants of $T_0 = 10\,497.37$ cm^{-1} , $\omega'_e = 397.85$ cm^{-1} , $\omega'_e x'_e = 3.39$ cm^{-1} , and $\Delta G''_{1/2} = 357.7$ cm^{-1} for $^{90}\text{Zr}^{59}\text{Co}$. Band positions as reported in Table I.

Without rotational resolution the assignment of term symbols to the upper and lower states of the transition is tentative at best. It should be noted, however, that the band

profiles of each of the four bands in this system are similar, and appear to consist of branches fanning out more or less symmetrically from the band origin, with no obvious Q branch features. Assuming that the ground state is indeed $X^2\Sigma^+$ (as in the other 13 electron metal molecules), such a profile is expected for a $2\Sigma^+ \leftarrow 2\Sigma^+$ transition, which for negligible spin splittings appears very similar to a $1\Sigma \leftarrow 1\Sigma$ transition. The other electric dipole allowed candidate for the transition, $2\Pi \leftarrow X^2\Sigma^+$, would be expected to display both $2\Pi_{1/2} \leftarrow X^2\Sigma^+$ and $2\Pi_{3/2} \leftarrow X^2\Sigma^+$ subbands, and corresponding vibrational features of these two subsystems would be expected to be of identical intensity, as is observed in the case of ScNi in Fig. 1. On the basis of these results, the band system displayed in Fig. 7 is tentatively identified as the $[10.5]^2\Sigma^+ \leftarrow X^2\Sigma^+$ system of ZrCo. In all likelihood our failure to rotationally resolve this band system given our laser linewidth of 0.04 cm^{-1} stems from unresolved hyperfine structure due to the interaction between the ^{59}Co nucleus ($I=7/2$) and the unpaired electron.

The excited state lifetime of the $[10.5]^2\Sigma^+$ state of ZrCo was measured to be $590 \pm 14 \text{ ns}$. Assuming that the upper state decays entirely by fluorescence to the ground state this corresponds to an absorption oscillator strength of $f \approx 0.025$, indicating a strongly allowed transition.

IV. DISCUSSION

The $X^2\Sigma^+$ ground state of the 13 electron molecules ScNi, YPd, and ZrCo may be represented by the molecular orbital configuration $1\sigma^2 2\sigma^2 1\pi^4 1\delta^4 3\sigma^{*1}$ following the molecular orbital numbering of Van Zee and Weltner.⁵ In this description the 1σ orbital is formed by overlap of the valence s orbitals on the two atoms and is strongly bonding in character. The 2σ , 1π , and 1δ orbitals are primarily d -based molecular orbitals which are more localized on the late transition metal atom, although some delocalization onto the early transition metal atom is of course expected (and required if d -orbital contributions to the bonding are to occur). The unpaired electron resides in the $3\sigma^*$ orbital, which may be considered the antibonding analog of the bonding 1σ orbital. According to Faegri and Bauschlicher this orbital is primarily s in character, although a significant amount of p character is mixed into the wave function.⁷

Although ScNi, YPd, and ZrCo all possess $X^2\Sigma^+$ ground states with similar bonding, the vibrational frequencies and force constants vary considerably across this series of molecules. Converting the measured vibrational intervals of these species, we find ground state force constants of 167 N/m for ScNi ($\Delta G''_{1/2} = 334.5 \text{ cm}^{-1}$), 201 N/m for YPd ($\Delta G''_{1/2} = 264.4 \text{ cm}^{-1}$), and 332 N/m for ZrCo ($\Delta G''_{1/2} = 357.7 \text{ cm}^{-1}$). Although the force constant and bond strength of a diatomic molecule are independent properties, a strong correlation exists between them. If there were a direct correspondence between force constant and bond strength this would suggest that ZrCo is the most strongly bound of these molecules.

In a previous paper we have reported a predissociation threshold measurement of the bond strength of ZrCo, giving $D_0^\circ(\text{ZrCo}) = 3.137 \pm 0.001 \text{ eV}$.² Bond strengths of YCo, YNi,

ZrNi, NbNi, NbCo, and Zr_2 were also reported in this paper, and it was found that ZrCo had the greatest bond strength of any of these molecules. Of particular relevance to the present study is that the bond strength of ZrCo is slightly greater than that of YNi, which was found to have $D_0^\circ(\text{YNi}) = 2.904 \pm 0.001 \text{ eV}$.² In their *ab initio* investigation of ScNi, ScPd, YNi, and YPd, however, Faegri and Bauschlicher found the bond strengths of the palladium compounds to be roughly 0.3 eV greater than those of the corresponding nickel compounds at the highest level of theory, suggesting that the true bond strength of YPd should be approximately 3.2 eV [$D_0^\circ(\text{YNi}) + 0.3 \text{ eV}$]. This estimate of the YPd bond strength is significantly greater than that measured by Knudsen effusion mass spectrometry [$D_0^\circ(\text{YPd}) = 2.46 \pm 0.16 \text{ eV}$].¹⁴ Although there are no obvious errors in the Knudsen effusion measurement, the predissociation threshold measurement of the YNi bond strength seems definitive, and it would be very surprising for YPd to have a weaker bond than YNi given the larger size and therefore greater accessibility of the d orbitals in palladium as compared to nickel. On this basis it seems that the bond strengths of YPd and ZrCo should be quite comparable, indicating that the larger force constant found for ZrCo does not reflect a greater bond strength.

A possible explanation for the larger force constant of ZrCo as opposed to YPd may be found in the concept of promotion energies. The ground states of Zr and Co are $4d^2 5s^2$, $3F$ and $3d^7 4s^2$, $4F$, respectively. These atoms cannot come together directly to form a bond because of Pauli repulsions between the filled s subshells. Instead, the ground state of the ZrCo molecule almost certainly requires that one atom be promoted to a $d^{n+1} s^1$ configuration. As cobalt requires less energy to promote than does zirconium, it is the cobalt promotion energy that is relevant. As described more fully in our paper on the bond strengths of YCo, YNi, ZrCo, ZrNi, NbCo, NbNi, and Zr_2 ,² this promotion energy occurs at the expense of the strength of the bond that is formed, in the case of ZrCo lowering the bond strength by approximately 0.65 eV. No corresponding atomic promotion is required to form YPd in its ground state, so its promotion energy is zero. Thus the intrinsic bond strength of ZrCo probably exceeds that of YPd by approximately 0.65 eV, and this is reflected in the larger force constant found for ZrCo. In contrast, the promotion energy of nickel is much less than that of cobalt, so the force constants of the ScNi and YPd molecules are comparable.

Another possible reason for the discrepancy in force constants between the (ScNi, YPd) molecules and ZrCo is that in ZrCo the distribution of d electrons on the two centers is not as severely polarized as in the former molecules. This leads to covalent d -orbital interactions as opposed to the more dative type of interactions that are required in ScNi and YPd. Given that dative donation of d electrons from the late to the early transition metal corresponds to electron donation from the more electronegative element to the more electropositive element, it may be expected to be disfavored. Thus the d -orbital contributions to the bonding in ZrCo are expected to be stronger than in YNi or ScPd, again leading to a considerably stronger force constant. To illustrate the magni-

tude of this effect, one may consider the ten valence electron molecules V_2 , VNb , and Nb_2 , which bond through covalent rather than dative d orbital interactions. Although these molecules have only ten valence electrons (thereby preventing full occupation of the nominally bonding $\delta_{(g)}$ orbitals), they nevertheless have force constants (and vibrational frequencies) of 434 N/m (537.5 cm^{-1}),¹⁷ 441 N/m (476.89 cm^{-1}),¹⁸ and 494 N/m (424.89 cm^{-1}),¹⁹ respectively. These are substantially greater than any of the 13-electron molecules considered here, supporting the idea that covalent d -orbital interactions are stronger than dative interactions.

A measure of the significance of the d orbital contributions to the bonding in the ScNi, YPd, and ZrCo molecules may be obtained by comparison to a related molecule where the d orbitals are expected to make a negligible contribution to the bond. One such molecule is YCu, where the small physical size and low orbital energy of the copper $3d$ orbitals makes them essentially inaccessible for chemical bonding. In this molecule it appears that substantial $4d-5s$ hybridization occurs on yttrium in its $5s^2 4d^1$, 2D ground state, allowing the formation of a $(4d\sigma-5s\sigma)_{Y-4s_{Cu}}$ sigma bond when it is combined with a ground state $3d^{10} 4s^1$, 2S copper atom, leading to a $^1\Sigma^+$ ground state in the resulting YCu molecule. The ground state vibrational frequency in $^{89}Y^{63}Cu$ has been measured as $\omega_e'' = 193.2 \text{ cm}^{-1}$, implying a force constant of 81.0 N/m.²⁰ The force constants of the three 13 valence electron species investigated in the present study, ScNi, YPd, and ZrCo, are all more than double that of YCu. This is indicative of strong d -orbital contributions to the bonding in all three species.

V. CONCLUSION

The optical spectra of ScNi, YPd, and ZrCo have been recorded from the visible to the near infrared. A single $^2\Pi \leftarrow X^2\Sigma^+$ band system has been observed in ScNi at $10\,100 \text{ cm}^{-1}$ and a single $^2\Sigma^+ \leftarrow X^2\Sigma^+$ band system has been found in ZrCo at $10\,500 \text{ cm}^{-1}$. In contrast, five band systems have been recorded for YPd over the frequency range from 6500 to $16\,000 \text{ cm}^{-1}$. Vibrational constants for the ground and excited states have been measured, along with excited state lifetimes. Vibrational intervals for the ground $^2\Sigma^+$ states are measured to be 334.5 , 264.4 , and 357.7 cm^{-1} for $^{45}Sc^{58}Ni$, $^{89}Y^{108}Pd$, and $^{90}Zr^{59}Co$, respec-

tively. These vibrational intervals are in excellent agreement with the results of *ab initio* quantum chemistry in the cases of ScNi and YPd, where high level theoretical calculations have been performed. Unfortunately, it has proven impossible to rotationally resolve these band systems with the laser linewidth of 0.04 cm^{-1} that is presently available in our laboratory, so a detailed comparison of bond lengths and excited state term symbols between theory and experiment must await a future investigation.

ACKNOWLEDGMENTS

We gratefully acknowledge research support from the National Science Foundation under Grant No. CHE-9215193. The donors of the Petroleum Research Fund, administered by the American Chemical Society are also acknowledged for partial support of this research.

- ¹N. Engel, *Acta Metall.* **15**, 557 (1967); L. Brewer, *Acta Metall.* **15**, 553 (1967); *Science* **161**, 115 (1968).
- ²C. A. Arrington, T. Blume, M. D. Morse, M. Doverstål, and U. Sassenberg, *J. Phys. Chem.* **98**, 1398 (1994).
- ³H. Wang and E. A. Carter, *J. Am. Chem. Soc.* **115**, 2357 (1993).
- ⁴R. J. Van Zee and W. Weltner, Jr., *High Temp. Sci.* **17**, 181 (1984).
- ⁵R. J. Van Zee and W. Weltner, Jr., *Chem. Phys. Lett.* **150**, 329 (1988).
- ⁶I. Shim and K. A. Gingerich, *Chem. Phys. Lett.* **101**, 528 (1983).
- ⁷K. Faegri, Jr. and C. W. Bauschlicher, Jr., *Chem. Phys.* **153**, 399 (1991).
- ⁸S. M. Mattar, and W. D. Hamilton, *J. Phys. Chem.* **96**, 8277 (1992).
- ⁹Z.-W. Fu, G. W. Lemire, Y. Hamrick, S. Taylor, J.-C. Shui, and M. D. Morse, *J. Chem. Phys.* **88**, 3524 (1988).
- ¹⁰S. Gerstenkorn and P. Luc, *Atlas du Spectre d'Absorption de la Molécule d'Iode* (CNRS, Paris, 1978); S. Gerstenkorn and P. Luc, *Rev. Phys. Appl.* **14**, 791 (1979).
- ¹¹P. R. Bevington, *Data Reduction and Error Analysis for the Physical Sciences* (McGraw-Hill, New York, 1969), CURFIT program, pp. 235–245.
- ¹²D. J. Clouthier and J. Karolczak, *Rev. Sci. Instrum.* **61**, 1607 (1990).
- ¹³E. M. Spain and M. D. Morse, *J. Phys. Chem.* **96**, 2479 (1992).
- ¹⁴E. S. Ramakrishnan, I. Shim, and K. A. Gingerich, *J. Chem. Soc. Faraday Trans. 2* **80**, 395 (1984).
- ¹⁵H. Lefebvre-Brion and R. W. Field, *Perturbations in the Spectra of Diatomic Molecules* (Academic, Orlando, 1986).
- ¹⁶L. M. Russon, G. K. Rothschof, P. B. Armentrout, and M. D. Morse (unpublished results).
- ¹⁷C. Cossé, M. Fouassier, T. Mejean, M. Tranquille, D. P. DiLella, and M. Moskovits, *J. Chem. Phys.* **73**, 6076 (1980).
- ¹⁸A. M. James, P. Kowalczyk, and B. Simard, *Chem. Phys. Lett.* **216**, 512 (1993).
- ¹⁹A. M. James, P. Kowalczyk, R. Fournier, and B. Simard, *J. Chem. Phys.* **99**, 8504 (1993).
- ²⁰C. A. Arrington, D. J. Brugh, M. D. Morse, and M. Doverstål, *J. Chem. Phys.* (to be submitted).